PNAS
www.pnas.org

Supplementary Information for

Inhibition of Dual-Specificity Tyrosine-phosphorylation Regulated Kinase 2 Perturbs 26S Proteasome-addicted Neoplastic Progression

Sourav Banerjee[1,14], Tiantian Wei[2,3,14], Jue Wang[4,14], Jenna J. Lee[5], Haydee L. Gutierrez[6], Owen Chapman[7], Sandra E. Wiley[1], Joshua E. Mayfield[1], Vasudha Tandon[1], Edwin F. Juarez[7], Lukas Chavez[7,8], Ruqi Liang[2,3], Robert L. Sah[5], Caitlin Costello[8,9], Jill P. Mesirov[7,8], Laureano de la Vega[10], Kimberly L. Cooper[6], Jack E. Dixon[1,11,12,*], Junyu Xiao[2,3,*], Xiaoguang Lei[3,4,13,*]

[*]Corresponding authors: Jack E. Dixon (jedixon@ucsd.edu); Junyu Xiao (junyuxiao@pku.edu.cn); Xiaoguang Lei (xglei@pku.edu.cn)

This PDF file includes:

MATERIALS & METHODS

Cell culture and lysis

Mammalian cells were all grown in a humidified incubator with 5% CO_2 at 37°C. HEK293T, MDA-MB-231, MDA-MB-468, and Hs578T cells were grown in Dulbecco's Modified Eagle Media (DMEM, Gibco) supplemented with 10% FBS, 1% L-glutamine, and 1% penicillin and streptomycin. RPMI8226, 8226.BR, MM.1S, MM.1S.BR, MM.1R, ANBL6, U266B1, HCC70, HCC1937, HCC1187, EO771, MPC11, and 5TGM1-GFP cells were grown in RPMI 1640 (Gibco) supplemented with 10% FBS, 1% L-glutamine, and 1% penicillin and streptomycin. AHH1 cells were cultured in RPMI-1640 with 10% horse serum, 10 mM HEPES, and 1.0 mM sodium pyruvate (Life Technologies). MCF10A and 184B5 cells were cultured in DMEM/F-12 medium supplemented with 5% horse serum, 20 ng/ml EGF, 0.5 μg/ml hydrocortisone, 100 ng/ml cholera toxin, 10 μg/ml insulin and 1% penicillin and streptomycin. FT190 and FT240 cells were cultured in DMEM/F-12 medium supplemented 10% FBS, 1% L-glutamine, and 1% penicillin and streptomycin. Post-treatment and/or transfection, cells were lysed in lysis buffer containing 50 mM Tris/HCl (pH 7.5), 1 mM EGTA, 1 mM EDTA, 1% Triton X-100, 50 mM NaF, 10 mM sodium 2-glycerophosphate, 5 mM sodium pyrophosphate, 1 mM sodium orthovanadate, 0.27 M sucrose, 1 mM benzamidine (added before lysis), 1 mM PMSF (added before lysis) and 0.1% β-mercaptoethanol (added before lysis). For proteasome pull-down or activity assays, cells were lysed in 50 mM Tris/HCl (pH 7.5), 0.1% Nonidet P-40, 1 mM ATP, 10 mM $MgCl_2$, 1 mM DTT and a phosphatase inhibitor cocktail (10 mM NaF, 20 mM β-glycerophosphate and 50 nM Calyculin A).

Proteasome activity assays

Proteasome activity assays were analysed either directly on cell lysates or on human 26S proteasome pulled-down from MDA-MB-468 cells stably expressing Rpn11-TBHA as described previously (1, 2). Cells were treated with or without indicated concentration of LDN192960 prior to lysis. Peptidase activities of purified proteasome or proteasomes in whole cell or tumor lysates were assayed using fluorogenic peptide substrates (Enzo Life Sciences) (3) with phosphatase inhibitors present in the lysis and assay buffers. The measured activity was normalized either against total protein concentration of cell lysates. Fluorescence signals were quantified using a Tecan plate reader.

Mouse allo/xenograft models

C57BL/6J, J:NU, and *NSG™* mice were purchased from the Jackson Laboratory. *BALB/c* inbred mice were purchased from Envigo. Mice were housed and maintained at the University of California-San Diego (UCSD) in full compliance with policies of the Institutional Animal Core and Use Committee (IACUC).

2.5-5 × 10^6 MM.1S or 8226 or 8226.BR cells were resuspended in 1:1 slurry with Matrigel™ and subcutaneously injected into the right flank of J:NU mice. Tumors were measured every 2-3 days using a caliper. Tumor volumes were calculated as volume=(width^2 × length) /2.

1-5 × 10^6 5TGM1-GFP or MPC11 cells were injected into the tail-vein of indicated mice. Mice were observed for movement difficulties and consequent hind-limb paralysis. For bone analyses, mice were euthanized post 3-5 weeks of injection. For the Kaplan-Meier curve, moribund mice with dual hindlimb paralysis was considered the 'end-point'. For all multiple myeloma models, mice of both gender 6-8 weeks old have been used.

For TNBC models, 0.2-0.5 × 10^6 MDA-MB-231 or EO771 cells were resuspended in 1:1 slurry with Matrigel™ and injected into the #4 mammary fat pad of J:NU (for MDA-MB-231) or C57BL/6J (for EO771) mice. For patient-derived xenograft TNBC model, 1-2 mm diameter tumor chunks of PDX97 were dipped into Matrigel™ and implanted subcutaneously on the neck of J:NU mice. Tumors were measured

every 2-3 days using a caliper. Tumor volumes were calculated as volume=(width^2 × length) /2. For all TNBC models, only female mice 6-8 weeks old have been used.
LDN192960 or PBS vehicle control treatment was started when tumors were either palpable or after 2 weeks of tail-vein injection. LDN192960 dissolved in sterile PBS was always injected intraperitoneally at a dose of 50 mg/Kg 3 times weekly unless otherwise specified.

CD138$^+$ myeloma cell and PBMC purification

Bone marrow aspirates and matched peripheral blood samples were obtained from HIPAA compliant de-identified consenting patients in accordance with Institutional Review Board approved protocols at University of California-San Diego (UCSD). Peripheral blood was processed by density centrifugation with Histoplaque-1077 in a SepMate50 conical tube (StemCell Technologies). CD138$^+$ primary myeloma cells were purified from fresh bone marrow aspirates of multiple myeloma patients using EasySep™ Human Whole Blood and Bone Marrow CD138 Positive Selection Kit II (StemCell Technologies) following manufacturer's instructions. Viable cells were collected for further analyses.

Histology

DYRK2 IHC was carried out on a breast cancer patient tissue array purchased from Biomax Inc, USA. The tissue array slide was baked at 60 ºC for 1 hour then dewaxed with Histo-Clear II (Cat HS-202). The dewaxed slide was rehydrated through a graded ethanol series (2 x 2 min in 100% EtOH, and 2 min each in 90% EtOH and 70% EtOH) and rinsed in distilled water. Antigen retrieval was performed by boiling the rehydrated slide for 6 minutes in Tris EDTA (pH=9) buffer (1mM EDTA, 10 mM Tris Base). The slide was then cooled at RT for 30 min, rinsed in distilled water, treated with 3% H_2O_2 and rinsed with distilled water. The slide was blocked with 1% normal goat serum (MP Biomedicals Cat 08642921) in TBS for 1 hour at RT then incubated with 1:200 dilution of rabbit polyclonal anti-DYRK2 antibody (Abgent) in TBS overnight at 4 ºC. Slide was washed 2 X 5 min in TBS then incubated with 1:500 dilution of goat Anti-Rabbit IgG (H+L) conjugated secondary antibody (Promega W401B) in TBS for 1 hour. Slide was then washed 2 x 5 min in TBS, developed in Signal Stain DAB Substrate Kit (Cell signaling Cat 8059Z) for 2 min, and then washed in running distilled water for 10 minutes. Slide was then dehydrated through a graded ethanol series, cleared in Histo-Clear II and mounted in Permount (Fisher SP15-100) under a glass coverslip.

Ki67 IHC was carried out at the UCSD Histology and Tissue Technology core. Tumor sections were embedded in paraffin and sections were mounted on slides. The slides were baked at 60 ºC for 1 hour then dewaxed with Histo-Clear II (Cat HS-202). Dewaxed slides were rehydrated through successive alcohols (3X Xylene, 2X 100% EtOH, 2x 95% EtOH, 2X 70% EtOH, distilled water). Antigen retrieval was carried out in Diva Decloaker (pH=6.2) (Biocare, DV2004 MX) at 95ºC for 30 min. Staining was performed on Intellipath Automated IHC Stainer (Biocare). Slides were treated for 10 min with peroxidase block Bloxall (Vector, SP-6000) then rinsed 2 x 5 min in TBS. Slides were blocked with Background Punisher (Biocare, BP974) for 10 min at RT then incubated with 1:200 dilution of rabbit anti-Ki67 antibody (GeneTex, Cat# GTX16667) for 1 hour. Slides were washed 2 X 5 min in TBS then incubated with 1:500 dilution of goat Anti-Rabbit IgG (H+L) conjugated secondary antibody (Biocare, RHRP520 L) for 30 min. Slide was then washed 2 x 5 min in TBS, developed in DAB (brown) Chromagen (Biocare, IPK5010 G80) for 5 min and then washed in running distilled water for 10 minutes. Slides were counterstained with Hematoxylin (Mayers) Counterstain for 5 min washed 2 x 5 min in TBS and 2 x 5 mins distilled water and mounted in Permount (Fisher SP15-100) under glass coverslips.

For tartrate resistant acid phosphatase (4) activity staining, femurs were decalcified in 20% EDTA, pH 8, for 21 days at 4 ºC. Decalcified femurs were then washed briefly in 1X PBS and dehydrated through

a graded ethanol series (20 min each in 25% and 50% EtOH in 1X PBS, 20 min in 75% EtOH in water, 1 hour each in 90% and 95% ethanol, 4.5 hours in 100% EtOH). Dehydrated femurs were then washed for 4.5 hours in Xylenes, and infiltrated for 4 hours in paraffin before mounting in paraffin (McCormick Paraplast Cat 39503002). We then sectioned femurs in transverse orientation at 15 um thickness with a Leica RM2165 microtome and placed sections on Superfrost Plus slides. All chemicals used to stain for tartrate resistant acid phosphatase (4) activity were purchased from Sigma. TRAP Basic Incubation Medium is comprised of 9.2 g sodium acetate anhydrous, 11.4 g L-(+) tartaric acid (Cat 228729), 950 ml distilled water, and 2.8 ml glacial acetic acid (Cat 695092) adjusted to pH 4.7-5.0 with glacial acetic acid or 5 M sodium hydroxide. Naphthol AS-BI phosphate substrate (Cat AC415310010) is dissolved at 20 mg per ml in ethylene glycol monoethyl ether (Cat 128082). Sections were stained for TRAP activity by placing slides in prewarmed TRAP staining solution mix [200 ml TRAP Basic Incubation Medium, 120 mg Fast Red Violet LB Salt (Cat F3381), and 1 ml Naphthol AS-BI phosphate substrate solution] at 37^{o}C for 30 minutes. Slides were then rinsed in distilled water, counterstained with 0.02% Fast Green (Cat F7252) for 90 seconds, and rinsed in distilled water. After dehydration through a graded series of EtOH, slides were cleared in Xylenes and mounted in Permount media (Cat SP15-100) under glass coverslips.

Synthesis and characterization of LDN192960

LDN192960 for co-crystallography was synthesized as par the reported procedure (5). All reagents were used as supplied by Sigma-Aldrich, J&K, Alfa Aesar Chemicals and TCI. NMR spectra were recorded on a Varian 400 MHz spectrometer, Bruker 400 MHz NMR spectrometer (ARX400) and Bruker 400 MHz NMR spectrometer (AVANCE III) at ambient temperature with MeOD-d4 as the solvent. Chemical shifts are reported in parts per million relative to MeOD-d4 (1H, δ 3.31; 13C, δ 49.00). Data for 1H NMR are reported as follows: chemical shift, integration, multiplicity (s = singlet, d = doublet, t = triplet, q = quartet, quint = quintet, sixt = sixtet, m = multiplet) and coupling constants. High-resolution mass spectra (HRMS) were obtained at Peking University Mass Spectrometry Laboratory using a Bruker APEX Flash chromatography. LDN192960 was purified by HPLC/MS on a Waters Auto Purification LC/MS system (ACQUITY UPLC BEH C18 17 μm 2.1X50 mm column). ^{1}H NMR (400 MHz, MeOD-d4) δ 8.06 (d, J = 9.4 Hz, 2H), 8.01 (d, J = 2.7 Hz, 2H), 7.52 (dd, J = 9.4, 2.7 Hz, 2H), 4.06(s, 6H), 3.12 (t, J = 7.6 Hz, 2H), 2.94 (t, J = 7.6 Hz, 2H), 1.78 (quint, J = 7.6 Hz, 2H). ^{13}C NMR (126 MHz, MeOD-d4) δ 160.46, 143.97, 139.52, 131.78, 128.53, 127.40, 103.50, 56.51, 39.46, 34.39, 29.39.; HRMS(EI) $[M+H]^{+}$ calculated for C18H21N2O2S: 329.1318, found: 329.1312.

DYRK2 protein purification and co-crystallization studies

DYRK2$^{208-552}$ or DYRK2 full length with an N-terminal 6×His affinity tag and TEV protease cleavage site which expressed in E. coli BL21 (DE3). Bacterial cultures were grown at 37 °C in LB medium to an OD600 of 0.6-0.8 before induced with 0.5 mM IPTG overnight at 18 °C. Cells were collected by centrifugation and frozen at -80 °C. For protein purification, the cells were suspended in the lysis buffer (50 mM HEPES, pH 7.5, 500 mM NaCl, 20 mM imidazole, 5% glycerol, 5 mM β-mercaptoethanol, and 1 mM phenylmethanesulfonylfluoride) and disrupted by sonication. The insoluble debris was removed by centrifugation. The supernatant was applied to a Ni-NTA column (GE Healthcare). The column was washed extensively with the wash buffer (50 mM HEPES, pH 7.5, 500 mM NaCl, 50 mM imidazole, 5% glycerol, and 5 mM β-mercaptoethanol) and bound DYRK2 protein was eluted using the elution buffer (50 mM HEPES, pH 7.5, 500 mM NaCl, 500 mM imidazole, 5% glycerol, and 5 mM β -mercaptoethanol). After cleavage with TEV protease, the protein sample was passed through a second Ni-NTA column to separate

untagged DYRK2 from the uncut protein and the protease. Final purification was performed using a Superdex 200 gel filtration column (GE Healthcare), and the protein was eluted using the final buffer (25 mM HEPES, pH 7.5, 400 mM NaCl, 1 mM DTT, and 5% glycerol). Purified DYRK2 was concentrated to 10 mg ml-1 and flash-frozen with liquid nitrogen.

$DYRK2^{208-552}$ was incubated with 200 μM LDN192960 on ice before crystallization. The protein-LDN192960 mixture was then mixed in a 1:1 ratio with the crystallization solution (0.36 M-0.5 M sodium citrate tribasic dihydrate, 0.01 M sodium borate, pH 7.5-9.5] in a final drop size of 2 μl. The DYRK2-LDN192960 crystals were grown at 18 °C by the sitting-drop vapor diffusion method. Cuboid-shaped crystals appeared after 4-7 days. Crystals were cryoprotected in the crystallization solution supplemented with 30% glycerol before frozen in liquid nitrogen. The X-ray diffraction data were collected at Shanghai Synchrotron Radiation Facility (SSRF) beamline BL17U. The diffraction data were indexed, integrated, and scaled using HKL-2000 (HKL Research). The structure was determined by molecular replacement using the published DYRK2 structure (PDB ID: 3K2L) (6) as the search model using the Phaser program (7). Chemdraw (version 15.0) was used to generated the .cif file for LDN192960, and then LDN192960 was fitted using the LigandFit program in Phenix (8). The structural model was further adjusted in Coot (9) and refined using Phenix. The quality of the structural model was checked using the MolProbity program in Phenix. The crystallographic data and refinement statistics are summarized in Table S1**.**

IC_{50} determination and kinase inhibitor specificity profiling

IC_{50} determination was carried out at The International Centre for Protein Kinase Profiling (http://www.kinase-screen.mrc.ac.uk/). Active DYRK1A, DYRK2, DYRK3, PIM3 and CK2 were purified as reported previously (10). LDN192960 IC_{50} measurements were carried out against the kinases with final concentrations between 0.1 nM to 10 μM *in vitro* (LDN192960 was added to the kinase reaction prior to ATP master mix). The values were expressed as a percentage of the DMSO control. DYRK isoforms (5-20 mU diluted in 50 mM Tris pH7.5, 0.1 mM EGTA, 0.1% β-mercaptoethanol) are assayed against Woodtide (KKISGRLSPIMTEQ) in a final volume of 25.5μl containing 50 mM Tris pH 7.5, 0.1 mM EGTA, 300 μM substrate peptide, 10 mM Magnesium acetate and 0.01-0.3 mM [^{33}P-γATP] (0.05 mM for DYRK1A and 0.005 mM for DYRK3) (50-1000 cpm/pmole) and incubated for 30 min at room temperature. PIM3 (5-20 mU diluted in 50 mM Tris pH 7.5, 0.1 mM EGTA, 0.1% β-mercaptoethanol, 1 mg/ml BSA) was assayed against a substrate peptide (RSRHSSYPAGT) in a final volume of 25.5 μl containing 50mM Tris pH 7.5, 0.05% b-mercaptoethanol, 300 μM substrate peptide, 10 mM magnesium acetate and 0.02 mM [^{33}P-γATP] (50-1000 cpm/pmole) and incubated for 30 min at room temperature. CK2 (5–20 mU diluted in 20 mM Hepes pH7.5, 0.15 M NaCl, 0.1 mM EGTA, 0.1% Triton X-100, 5 mM DTT, 50% glycerol) was assayed against CKII peptide (RRRDDDSDDD) in a final volume of 25.5 μl containing 20 mM Hepes pH 7.5, 0.15 M NaCl, 0.1 mM EDTA, 5 mM DTT, 0.1% Triton-X 100, CKII peptide (0.165 mM), 10 mM magnesium acetate and 0.005 mM [^{33}P-γATP](500 -1000 cpm/pmole) and incubated for 30 min at room temperature. Assays are stopped by addition of 5 μl of 0.5 M (3%) orthophosphoric acid and then harvested onto P81 Unifilter plates with a wash buffer of 50 mM orthophosphoric acid. IC_{50} curves were developed as % of DMSO control and IC_{50} values were calculated using GraphPad Prism software.

Kinase inhibitor specificity profiling assays were carried out at The International Centre for Protein Kinase Profiling (http://www.kinase-screen.mrc.ac.uk/). LDN192960 kinase specificity was determined against a panel of 140 protein kinases as described previously (2, 10, 11). The assay mixes and ^{33}P-γATP were added by Multidrop 384 (Thermo). Results are presented as a percentage of kinase activity in DMSO

control reactions. Protein kinases were assayed *in vitro* with 1 μM final concentration of LDN192960 and the results are presented as an average of triplicate reactions ± SD or in the form of comparative histograms.

ATP competition assay

Initial reaction velocities were determined by the addition 6.25 μL of 4X ATP stock solutions (50mM Tris-HCl pH 7.5, 40mM Magnesium Acetate, 0.04-1.2mM ATP supplemented with a constant ratio of trace [^{32}P-γATP] to 18.75 μL of pre-incubated kinase/inhibitor solution (50mM Tris-HCl, 0.13 mM EDTA, 400 μM Woodtide substrate, 11 ng/μL full length DYRK2, 0-1333nM LDN192960) to give a final 25 μL reaction volume containing 50mM Tris-HCl pH 7.5, 0.1mM EDTA, 10mM Magnesium Acetate, 300 μM Woodtide substrate, 8 ng/μL DYRK2, 0-1000nM LDN192960, 0.01-0.3mM ATP supplemented with a constant ration of trace [^{32}P-γATP]. Reactions were incubated at 30°C for 4 minutes and quenched through the addition of 6.3 μL 3% phosphoric acid. Reactions were spotted on Whatman P81 paper and washed three times with 1% phosphoric acid for 5 minutes each and once with 100% acetone for 10 minutes. P81 papers were transferred to scintillation vials and 32P CPM values were determined via scintillation counting in a Beckman LS 6000IC instrument. Background was determined from paired reactions containing no substrate peptide. Velocities were determined from background adjusted CPM values. Nonlinear regression to determine Michaelis-Menten constants was performed in R utilizing the nls() function. Lineweaver-Burke curves were determined by reciprocal transformation of Michaelis-Menten fits.

Cell transfection

Transient transfection of HEK293T and MDA-MB-231 cells was carried out using Lipofectamine 2000 (Life Technologies) as recommended by the manufacturer. Stable overexpression of DYRK2 and Rpn11-TBHA were carried out by Retroviral transduction followed by puromycin selection as reported previously (1). For shRNA lentivirus production, HEK293T cells were transfected at 80-90% confluency using Lipofectamine 2000 and psPAX2 and pMD2.G packaging vectors. Medium was changed 6-8 hours after transfection and supernatant was collected after 48-72 hr. Viral media was passed through a pre-wetted 0.8-mm PVDF filter (Millipore) and mixed with 8 μg ml^{-1} Polybrene (Sigma Aldrich) before being added to recipient 5TGM1-GFP cells. Infected cells were treated with G418 to generate stable populations.

Nucleofection of MM.1S, MPC11, and 5TGM1-GFP cells were carried out by AMAXA™ nucleofector II device (Lonza) using homemade nucleofection solutions. Solution 1 (0.4 M ATP, 0.5 M $MgCl_2.6H_2O$) was added fresh to Solution 2 (100 mM KH_2PO_4 , 15 mM $NaHCO_3$, 2 mM glucose) in the ratio of 1:50 prior to each nucleofection experiment. 5 μg of plasmid was added to 0.5-2 million cells in a final volume of 100 μL in the Solution 1+2 mixture. Amaxa™ protocol O-023 was used for all 3 cell lines. The mixed Solution 1+2 was never stored post-procedure.

Genome editing

Genome editing was carried out by Crispr/Cas9 via a pool of 2-4 guide RNAs. Briefly, MDA-MB-231 cells were transfected with a pool of 2 guide RNAs using pX458 vector expressing GFP. Multiple myeloma cells MM.1S, MPC11, and 5TGM1-GFP cells were transfected with a pool of 4 guide RNAs using pL-CRISPR.EFS.tRFP vector expressing RFP. Positive population of cells carrying the GFP/RFP were enriched by flow cytometry and cell sorting using BD FacsJazz. Knockout was determined by DNA sequencing and western blot. Crispr knock-out for myeloma cells and MDA-MB-231 were carried out fresh every time before experiments and never frozen.

Cell proliferation, viability and invasion assays

To measure cell proliferation, actively proliferating cells were seeded at a density of 1.0×10^5 cells/ml of media. Every 24 hours afterwards, cell numbers per ml of media were quantified using the Countess® automated cell counter (Life Technologies) for a total of 6 days. For MDA-MB-468 cell proliferation, 6×10^4 cells were plated in 96 well plates and proliferation assay was ascertained as fold proliferation using CellTiter 96® AQueous Non-Radioactive Cell Proliferation Assay kit following manufacturer's instructions. The time course experiments were repeated three times for each cell type. Cell proliferation assays were carried out either on parental or genome-edited or in the presence or absence LDN192960 of indicated concentrations. Media containing LDN192960 or DMSO control was replaced every 2 days to avoid excess degradation in cell culture media. Cell viability assays were carried out with or without 48 hr treatment of LDN192960 using the CellTiter 96® AQueous Non-Radioactive Cell Proliferation Assay kit following manufacturer's instructions and data was represented as %viability compared to DMSO treated control. The Matrigel invasion assay was performed using 8 μm pore size transwells coated with Matrigel™ (BD Biosciences) as described previously (2, 11). The bottom chamber contained normal growth media (DMEM with 10% FBS with or without 3 μM curcumin or LDN192960) as a chemoattractant. MDA-MB-231 cells were seeded into the upper chamber (20,000 cells/insert) in DMEM with 1% BSA with or without 3 μM curcumin or LDN192960. After 24 hr of culture, cells that migrated through the matrix were quantified using Cyquant following manufacturer's instructions (Life Technologies).

3D cell culture growth assay

The effect of LDN192960 on growth of MDA-MB-468, EO771, and MDA-MB-231 cells in three-dimensional culture was assessed using a methylcellulose assay following established protocols (12). Cells (10,000) were diluted in growth media and embedded in 1% methylcellulose (R&D, HSC001). Cell suspensions were mixed on a rotator for 15 min at RT before plating onto poly-hydroxyethyl methacrylic acid (poly-HEMA) 6 well plates (Costar). Drug treatments (1 μM or 3 μM LDN192960 or DMSO vehicle control) were added during mixing. Cells were transferred to a cell culture incubator and grown under standard conditions for 2-4 weeks, depending on cell type. Brightfield images were captured on an Olympus CKX41 inverted light microscope equipped with a DP12 digital camera (5 different fields for each well). Images were analyzed to determine total area of cell growth using Image J software. Experiments were performed in triplicate and repeated at least 2 times. Data were plotted using GraphPad Prism.

Micro Computed Tomography (μCT) imaging and data analysis

Femurs from MPC11/BALB/c allograft mice were fixed in 10% formalin for 24 hr and washed 2x in PBS. The femurs were imaged with a micro-computed tomography scanner, Skyscan 1076 (Kontich, Belgium). Each sample was wrapped in paper tissue that was moistened with PBS, and scanned at 9 μm voxel size, applying an electrical potential of 50 kVp and current of 200 μA, using a 0.5 mm aluminum filter. Mineral density was determined by calibration of images against 2 mm diameter hydroxyapatite rods (0.25 and 0.75 gHA/cm^3). A beam hardening correction algorithm was applied prior to image reconstruction. Image data was visualized for each sample with Dataviewer and CTAn (Kontich, Belgium). A series of 2-D transaxial slices were generated over various regions of the femur. Fifteen slices were distributed around the center slice position with a separation of 0.06 mm for the metaphysis and mid-diaphysis regions, and 0.03 mm for the proximal femur region. Trabecular bone analysis was performed as appropriate for skeletally-mature animals (13). The trabecular region was selected by automatic contouring

as close as possible to the periosteum but without overlapping the cortical bone. An adaptive threshold (using the mean maximum and minimum pixel intensity values of the surrounding ten pixels) was used to identify trabecular bone. From this region of trabecular bone, the following parameters were determined: tissue volume (TV), Trabecular bone volume (BV), trabecular bone volume fraction (% BV/TV), trabecular number (Tb.N), and bone mineral density (BMD). The technical quality of the image cross-sections was checked for damage before quantitative analysis was performed. Damaged areas were strictly avoided and never included in any quantitative analyses. Outliers were verified for legitimacy by checking the scan and reconstruction log file, image rotation, selection of the tip of growth plate, number of slices in metaphysis and diaphysis, and the contours.

Differential gene-expression analyses

Gene expression data (Fragments Per Kilobase of transcript per Million mapped reads, FPKM-normalized expression values derived from RNA-sequencing) was obtained from TCGA (NCI Genomic Data Commons portal) for BRCA patients using the module TCGAImporter from GenePattern (14). The resulting gene expression table across all BRCA samples together with a phenotype description and other meta information are available via the link in the Key Resources Table. Clinical annotation of BRCA patients was obtained from the annotation file "nationwidechildrens.org_clinical_patient_brca.txt" available at the NCI Genomic Data Commons portal. 115 TNBC samples were identified by selecting for samples with negative status on the fields "er_status_by_ihc", "pr_status_by_ihc", and "her2_status_by_ihc". FPKM gene expression values for genes DYRK2, RPT3 and PSMB5 were log2-transformed and plotted using the Seaborn Python visualization library. Statistical comparison of means between tumor and normal samples was performed using an adaptation of the Student's t-test for semi-paired samples (15).

MM quantile-normalized expression data from the Affymetrix Human Genome U133 Plus 2.0 microarray were obtained for CD138-selected bone marrow plasma cells from normal and patient donors from the Gene Expression Omnibus (GEO), dataset accession number GSE6477 (16, 17). Relative expression values were imported into the NCBI Geo2R web analysis platform and sorted by sample name into Normal (n=15), MGUS (n=22), Smoldering (n=24), Newly Diagnosed (n=73) and Relapsed (n=28) MM progression states. Pairwise differential expression analysis was performed between normal and each non-normal progression stage using *limma* (Ritchie et al., 2015). Expression values for DYRK2 (202970_at), PSMB5 (208799_at) and RPT3 (201252_at) were extracted. Normalized expression values were log-transformed and plotted using the Seaborn Python visualization library.

GFP$^+$ foci counting on femurs

5TGM1-GFP cells bearing NSG^{TM} mice were euthanized and femurs were rapidly excised, roughly cleaned, and number of GFP$^+$ foci was counted under a Leica M165 FC dissecting microscope with fluorescence. Number of foci per bone was counted for 6 femurs per cell strain. Representative images were taken in the same dissection microscope.

qRT-PCR

For qRT-PCR analysis, total RNA from 5TGM1-GFP cells were isolated using the NucleoSpin RNA kit (MACHEREY-NAGEL, Bethlehem, PA). cDNA was synthesized using the iScript kit (Bio-Rad). qRT-PCR analysis was performed using the SYBR® Premix Ex Taq™ II (Takara) on Applied Biosystems

7500 Real-Time PCR System. Data were normalized to corresponding GAPDH levels. Primer details in Key Resources table.

Cell cycle analyses

Cell cycle analyses using propidium iodide and flow cytometry were carried out as described previously (18). Asynchronous MM.1S cells were treated with either DMSO or LDN192960 at 10 μM for 4 hr. Post treatment, cells were washed with PBS+1% FBS and resuspended in flow cytometry tubes. Cells were then fixed by 1% paraformaldehyde and permeabilized with 90% ice-cold methanol and stored at −20°C until analysis. After washing fixed cells once with PBS+1% FBS, RNaseA (10 μg/ml) and propidium iodide (50 μg/ml) were added to the cells and incubated in the dark at room temperature (25°C) for 15 min. The live cell populations were then subjected to quantitative measurement of DNA content by flow cytometry using a FACSJAZZ™ (BD Biosciences) and cell cycle distribution and the percentage of G_2/M–S–G_1 cells to the total cells in tube were determined by the BD FACS™ Sortware software. Stacked bar graphs were derived using Graphpad Prism.

Statistics and data presentation

Details of all statistical tests and multiple comparisons used to derive p value has been detailed in Figure Legends. All experiments were repeated 2-3 times with multiple technical replicates to be eligible for the indicated statistical analyses, and representative image has been shown. All results are presented as mean ± SD unless otherwise mentioned. For animal studies, statistical power analysis was used to predetermine sample size. Effect size (Cohen's d) was estimated from smaller pilot experiments using the R package *effsize*. Power analysis was performed in the R package *pwr* utilizing estimated Cohen's d, a significance level of 0.05, and power of 0.8. Mice bearing parental tumors were randomized into two equal groups prior to vehicle or drug treatment. The investigators were not blinded to allocation during experiments and outcome assessment. Data were analysed using Graphpad Prism or *limma* statistical package.

MATERIALS

REAGENT or RESOURCE	SOURCE	IDENTIFIER
Antibodies		
Anti-p-Rpt3 (Thr25)	Dixon laboratory (1)	N/A
Anti-Rpt3/S6b subunit monoclonal antibody (TBP7-27)	Enzo lifesciences	Cat#: BML-PW8765-0100
Anti-Proteasome 20S monoclonal antibody (MCP231)	Enzo lifesciences	Cat#: BML-PW8195-0100
Anti-DYRK2 Antibody	Cell Signaling	Cat#: 8143
Anti-GAPDH (6C5)	Calbiochem	Cat#: CB1001500UG
Anti-DYRK2 Antibody (N-term) for IHC	Abgent	Cat#: AP7534a
Anti-IκBα Antibody	Cell Signaling	Cat#: 9242
Anti-p27 Kip1 Antibody	Cell Signaling	Cat#: 3686
Anti-Mouse secondary HRP	GE healthcare	Cat#: NXA931
Anti-Rabbit secondary HRP	GE healthcare	Cat#: NA934V
Anti-Rabbit IgG (H+L) conjugated for IHC	Promega	Cat#: W401B
Anti-Rabbit IgG (H+L) conjugated for IHC	Biocare	Cat#: RHRP520 L
Anti-Ki67	GeneTex	Cat#: GTX16667
Bacterial Strains		
One Shot™ TOP10 Chemically Competent *E. coli*	ThermoFisher Scientific	Cat#: C404010
E. coli BL21 (DE3)	Transgen Biotech	Cat#: CD601-03
Biological Samples		
Human breast cancer tissue array	US Biomax, Inc.	Cat#: BC081120d
Fresh frozen Triple-negative breast cancer PDX sample	UCSD Moores Cancer Centre Biorepository	Cat#: TM00097 (PDX97)
Primary human myeloma patient bone marrow aspirate and peripheral blood	Dr. Caitlin Costello (UCSD Moores Cancer Centre)	N/A
Chemicals, Peptides, and Recombinant Proteins		
Premier screen purified kinase library and substrate peptides	International Centre for Protein Kinase Profiling	http://www.kinase-screen.mrc.ac.uk/services/premier-screen
Purified recombinant DYRK2 [3-528]	mrcppureagents	Cat#: DU653
Purified recombinant DYRK2 [208-552]	This paper	N/A
Purified recombinant DYRK2 [full length]	This paper	N/A
SUC-LLVY-AMC	UBPBio	Cat#: G1100
Proteasome substrate pack	Enzo lifesciences	Cat#: BML-PW9905-0001
Woodtide substrate peptide: KKISGRLSPIMTEQ	Genscript (19)	N/A
^{33}P-γATP	Hartmann	Cat#: FF-301T
^{32}P-γATP	Perkin Elmer	Cat#:BLU002Z001MC
Calyculin A	Cell Signaling	Cat#: 9902
Cell culture		
Lipofectamine 2000	Invitrogen	Ref#: 11668-019
Dulbecco's Modified Eagle Medium (DMEM)	Gibco	Cat#: 11965-092
Fetal Bovine Serum	Sigma-Aldrich	Cat#: F8067-500ML

Horse Serum	Invitrogen	Cat#: 26050088
RPMI 1640 Medium	Gibco	Cat#: 11875093
Trypan Blue 0.4%	Gibco	Cat#: 15250061
Trypsin-EDTA (0.25%)	Gibco	Cat#: 25200-056
Penicillin/Streptomycin	Gibco	Ref#: 15140-122
Ampicillin, Sodium Salt	Sigma-Aldrich	Cat#: A9518-100G
Puromycin	Gibco	Ref#: A11138-03
G418	Gibco	Cat#: 10131027
Cycloheximide	Sigma-Aldrich	Cat#: C7698
Opti-MEM	Gibco	Cat#: 31985070
Histopaque®-1077	Sigma	Cat#: 10771-100ML
Matrigel™ Basement Membrane Matrix	BD Biosciences	Cat#: 354234
Biocoat Matrigel™ cell invasion assay inserts	BD Biosciences	Cat#: 354480
Methylcellulose	R&D	Cat#: HSC001
Poly-HEMA coated plates	Costar	
Propidium iodide	Molecular Probes	Cat#: P-3566
RNaseA	ThermoFisher Scientific	Cat#: EN0531
Histology		
Histo-Clear II	National Diagnostics	Cat#: HS-202
Goat Serum	MP Biomedicals	Cat#: 08642921
Signal Stain DAB Substrate Kit	Cell Signaling	Cat#: 8059Z
Permount	Fisher	Cat#: SP15-100
Diva Decloaker	Biocare	Cat#: DV2004 MX
Bloxall	Vector	Cat#: SP-6000
Background Punisher	Biocare	Cat#: BP974
DAB (brown) Chromagen	Biocare	Cat#: IPK5010 G80
Paraffin	McCormick Paraplast	Cat#: 39503002
L-(+) tartaric acid	Sigma	Cat#: 228729
Naphthol AS-BI phosphate substrate	Sigma	Cat#: AC415310010
Ethylene glycol monoethyl ether	Sigma	Cat#: 128082
Fast Red Violet LB Salt	Sigma	Cat#: F3381
Fast Green	Sigma	Cat#: F7252
Protein purification		
Ni-NTA	GE Healthcare	Cat#: 17526802
Superdex 200	GE Healthcare	Cat#: 17517501
TEV protease	Xiao laboratory	N/A
RNA		
SYBR® Premix Ex Taq™ II (Tli RNaseH Plus), Bulk	Takara	Cat#: RR820L
NucleoSpin® RNA II	Macherey-Nagel	Cat#: 740955.25
iScript™ cDNA Synthesis Kit	Bio-Rad	Cat#: 170-8891
Isopropanol	Acros Organics	Cat#: 42383-0040
Ethanol, 200 Proof Pure	Koptec	Product: V1016

Cloning		
Quick-gDNA Miniprep Kit	Zymo	Cat#: 11-317B
GeneJET Plasmid Miniprep Kit	Invitrogen	Cat#: K0503
NucleoBond® Xtra Maxi	Macherey-Nagel	Cat#: 740414.100
Zymoclean Gel DNA Recovery Kit	Zymo	Cat#: 11-301
T4 DNA Ligase Buffer	NEB	Cat#: B0202S
T4 DNA Ligase	NEB	Cat#: M0202S
BsmbI Restriction Enzyme	NEB	Cat#: R0580S
BbsI Restriction Enzyme	NEB	Cat#: R0539S
NEBuffer 3.1	NEB	Cat#: B7203S
NEBuffer 2.1	NEB	Cat#: B7202S
Treatment		
Bortezomib	Selleckchem	Cat#: S1013
LDN-192960 dihydrochloride	Sigma-Millipore	Cat#: SML0755
LDN-192960 dihydrochloride	Aobious Inc.	Cat#: AOB1696
Curcumin	Sigma-Millipore	Cat#: 08511
Dimethyl sulfoxide (DMSO)	Sigma-Millipore	Cat#: 472301
Carfilzomib	Selleckchem	Cat#: S2853
Ixazomib	Selleckchem	Cat#: S2180
Critical Commercial Assays		
CellTiter 96® AQueous One Solution Cell Proliferation Assay (MTS)	Promega	Cat#: G3581
EasySep™ Human Whole Blood and Bone Marrow CD138 Positive Selection Kit II	Stemcell Technologies	Cat#: 17887A
SepMate™-50	Stemcell Technologies	Cat#: 85450
CellEvent™ Caspase-3/7 Green Detection Reagent	ThermoFisher Scientific	Cat#: C10423
Deposited Data		
TCGA FPKM-normalized expression	https://datasets.genepattern.org/?prefix=data/TCGA_HTSeq_FPKM/BRCA/	N/A
DYRK2-LDN192960 co-crystal structure	PDB	PDB ID: 6K0J
Experimental Models: Cell Lines		
Mouse: MPC11	ATCC	Cat#: CCL-167
Mouse: 5TGM1-GFP	Babatunde Oyajobi (UT San Antonio)	(20)
Mouse: EO771	Richard Klemke (UC San Diego)	N/A
Human: PBMC	ATCC	Cat#: PCS-800-011
Human: U266B1	ATCC	Cat#: TIB-196
Human: RPMI8226	ATCC	Cat#: CCL-155
Human: MM.1R	ATCC	Cat#: CRL-2975
Human: MM.1S	ATCC	Cat#: CRL-2974
Human: 184B5	ATCC	Cat#: CRL-8799

Human: ANBL6	Robert Orlowski (MD Anderson Centre)	N/A
Human: AHH1	ATCC	Cat#: CRL-8146
Human: MDA-MB-231	Michael Karin (UC San Diego)	N/A
Human: MDA-MB-468	Michael Karin (UC San Diego)	N/A
Human: Hs578T	Alexandra Newton (UC San Diego)	N/A
Human: MCF10A	Alexandra Newton (UC San Diego)	N/A
Human: HCC70	ATCC	Cat#: CRL-2315
Human: HCC1937	ATCC	Cat#: CRL-2336
Human: HCC1187	ATCC	Cat#: CRL-2322
Human: RPMI8226.BR	Apollina Goel (U of Iowa)	(21)
Human: MM.1S.BR	Apollina Goel (U of Iowa)	(21)
Human: HEK293T	ATCC	Cat#: CRL-3216
Human: FT190	Robert Rottapel (Princess Margaret Cancer Center)	N/A
Human: FT240	Robert Rottapel (Princess Margaret Cancer Center)	N/A
Human: MDA-MB-468 DYRK2 KO	(1)	N/A
Human: MDA-MB-468 RPT3 T25A KI	(1)	N/A
Experimental Models: Mouse strains		
C57BL/6J inbred mice	The Jackson Laboratory	Stock No: 000664
J:NU athymic nude mice	The Jackson Laboratory	Stock No: 007850
NOD.Cg-*Prkdc*^{scid} *Il2rg*^{tm1Wjl}/SzJ (NSG)	The Jackson Laboratory	Stock No: 005557
BALB/c inbred mice	Envigo/Harlan	Strain: BALB/cAnNHsd
Oligonucleotides		
Crispr/Cas9 gRNA targeting sequence 1: *hDYRK2* GGACAGCATTCATAGACGGC	(1)	
Crispr/Cas9 gRNA targeting sequence 2: *hDYRK2* CCTGGATCTGTCCGTGAGCG	(1)	
Crispr/Cas9 gRNA targeting sequence 1: *mDYRK2* CTCGCTCGACCCGCCGGGTT	This paper	
Crispr/Cas9 gRNA targeting sequence 2: *mDYRK2* GCCGCCTACCCGACCGGTAA	This paper	
Crispr/Cas9 gRNA targeting sequence 3: *mDYRK2* TCGCTCGACCCGCCGGGTTC	This paper	
Crispr/Cas9 gRNA targeting sequence 4: *mDYRK2* GAACCCGGCGGGTCGAGCGA	This paper	

shRNA targeting oligo sequence: *mDYRK2* Forward:CCGGGTGCTTGGATGCTTTGCACAACTCGAG TTGTGCAAAGCATCCAAGCACTTTTTG; Reverse:AATTCAAAAAGTGCTTGGATGCTTTGCACAA CTCGAGTTGTGCAAAGCATCCAAGCAC	This paper	
Primer: *mDYRK2* Forward*:* TTAACCAGGAAACCTTCGGC; Reverse: GGGAGGCTTTTACCTTCCCC	This paper	
Primer: *mGAPDH* Forward*:* CACCATCTTCCAGGAGCGAG; Reverse: CCTTCTCCATGGTGGTGAAGAC	(22)	
Crispr/Cas9 surveyor primer: *mDYRK2* Forward*:* CTCCCGAGCGAGTGGGTC; Reverse: TTAAGTTCGCGACCCGGC	This paper	
Recombinant DNA		
pL-CRISPR.EFS.tRFP	Addgene	Cat#: 57819
pSpCas9(BB)-2A-GFP (PX458)	Addgene	Cat#: 48138
pLKO.1-neo	Addgene	Cat#: 13425
pQXIP-FLAG-DYRK2	Dixon laboratory (1)	N/A
pQXIP-RPN11-TBHA	Dixon laboratory (1)	N/A
Software and Algorithms		
GraphPad Prism 6	GraphPad	https://www.graphpad.com/data-analysis-resource-center/
MacVector 12.7.3	MacVector, Inc.	https://macvector.com/
HKL-2000	HKL Research	
Phaser	(7)	
Phenix	(8)	
Chemdraw	ChemBioDraw 15	http://www.chemdraw.com.cn
Coot	(9)	
Limma	(23)	
Dataviewer and CTAn		
ImageJ	NIH	https://imagej.nih.gov/ij/download.html
BD FACS Sortware	BD	N/A
TCGAImporter GenePattern Module	https://cloud.genepattern.org/gp/pages/index.jsf?lsid=urn:lsid:broad.mit.edu:cancer.software.genepattern.module.analysis:00369:5.2	N/A
Geo2R	NCBI	https://www.ncbi.nlm.nih.gov/geo/geo2r/
Seaborn: statistical data visualization	Michael Waskom	https://seaborn.pydata.org/
R: A language and environment for statistical computing.	R Core Team	https://www.R-project.org/
effsize: Efficient Effect Size Computation	Torchiano M	https://CRAN.R-project.org/package=effsize

pwr: Basic Functions for Power Analysis	Champely et al.	https://cran.r-project.org/web/packages/pwr/

SI REFERENCES

1. X. Guo *et al.*, Site-specific proteasome phosphorylation controls cell proliferation and tumorigenesis. *Nature cell biology* **18**, 202-212 (2016).
2. S. Banerjee *et al.*, Ancient drug curcumin impedes 26S proteasome activity by direct inhibition of dual-specificity tyrosine-regulated kinase 2. *Proceedings of the National Academy of Sciences of the United States of America* **115**, 8155-8160 (2018).
3. A. F. Kisselev, A. L. Goldberg, Monitoring activity and inhibition of 26S proteasomes with fluorogenic peptide substrates. *Methods in enzymology* **398**, 364-378 (2005).
4. K. Huber *et al.*, 7,8-Dichloro-1-oxo-beta-carbolines as a Versatile Scaffold for the Development of Potent and Selective Kinase Inhibitors with Unusual Binding Modes. *Journal of Medicinal Chemistry* **55**, 403-413 (2012).
5. G. D. Cuny *et al.*, Structure-activity relationship study of acridine analogs as haspin and DYRK2 kinase inhibitors. *Bioorganic & medicinal chemistry letters* **20**, 3491-3494 (2010).
6. M. Soundararajan *et al.*, Structures of Down syndrome kinases, DYRKs, reveal mechanisms of kinase activation and substrate recognition. *Structure (London, England : 1993)* **21**, 986-996 (2013).
7. A. J. McCoy *et al.*, Phaser crystallographic software. *Journal of applied crystallography* **40**, 658-674 (2007).
8. P. D. Adams *et al.*, PHENIX: a comprehensive Python-based system for macromolecular structure solution. *Acta crystallographica. Section D, Biological crystallography* **66**, 213-221 (2010).
9. P. Emsley, B. Lohkamp, W. G. Scott, K. Cowtan, Features and development of Coot. *Acta crystallographica. Section D, Biological crystallography* **66**, 486-501 (2010).
10. J. Bain *et al.*, The selectivity of protein kinase inhibitors: a further update. *The Biochemical journal* **408**, 297-315 (2007).
11. S. Banerjee *et al.*, Characterization of WZ4003 and HTH-01-015 as selective inhibitors of the LKB1-tumour-suppressor-activated NUAK kinases. *Biochemical Journal* **457**, 215-225 (2014).
12. I. Tancioni *et al.*, FAK activity protects nucleostemin in facilitating breast cancer spheroid and tumor growth. *Breast Cancer Res* **17**, 47 (2015).
13. M. L. Bouxsein *et al.*, Guidelines for assessment of bone microstructure in rodents using micro-computed tomography. *Journal of bone and mineral research : the official journal of the American Society for Bone and Mineral Research* **25**, 1468-1486 (2010).
14. M. Reich *et al.*, GenePattern 2.0. *Nat Genet* **38**, 500-501 (2006).
15. B. Derrick, Russ, B., Toher, D., & White, P, Test statistics for the comparison of means for two samples that include both paired and independent observations. *Journal of Modern Applied Statistical Methods* **16(1), 137-157** (2017).
16. W. J. Chng *et al.*, Molecular dissection of hyperdiploid multiple myeloma by gene expression profiling. *Cancer Res* **67**, 2982-2989 (2007).

17. R. E. Tiedemann *et al.*, Kinome-wide RNAi studies in human multiple myeloma identify vulnerable kinase targets, including a lymphoid-restricted kinase, GRK6. *Blood* **115**, 1594-1604 (2010).
18. S. Banerjee *et al.*, Interplay between Polo kinase, LKB1-activated NUAK1 kinase, PP1 beta(MYPT1) phosphatase complex and the SCF beta TrCP E3 ubiquitin ligase. *Biochemical Journal* **461**, 233-245 (2014).
19. Y. L. Woods *et al.*, The kinase DYRK phosphorylates protein-synthesis initiation factor eIF2Bepsilon at Ser539 and the microtubule-associated protein tau at Thr212: potential role for DYRK as a glycogen synthase kinase 3-priming kinase. *The Biochemical journal* **355**, 609-615 (2001).
20. B. O. Oyajobi *et al.*, Detection of myeloma in skeleton of mice by whole-body optical fluorescence imaging. *Molecular cancer therapeutics* **6**, 1701-1708 (2007).
21. K. Salem, M. L. McCormick, E. Wendlandt, F. Zhan, A. Goel, Copper-zinc superoxide dismutase-mediated redox regulation of bortezomib resistance in multiple myeloma. *Redox biology* **4**, 23-33 (2015).
22. A. J. Pollak *et al.*, A secretory pathway kinase regulates sarcoplasmic reticulum Ca(2+) homeostasis and protects against heart failure. *eLife* **7** (2018).
23. M. E. Ritchie *et al.*, limma powers differential expression analyses for RNA-sequencing and microarray studies. *Nucleic Acids Res* **43**, e47 (2015).

SUPPLEMENTARY TABLES

Cancer type	Tumor (n)	normal (n)	Derrick's p-value	t-test p-value
ACC	79	0		
BLCA	408	19	0.000246637	0.000251589
BRCA_TN	115	11	0.019188774	0.028281101
BRCA	976	102	1.84E-08	3.23E-07
CESC	304	3	0.627008816	0.227287301
CHOL	36	9	2.24E-14	8.66E-17
COAD	456	41	8.04E-13	2.22E-13
DLBC	48	0		
ESCA	161	11	0.003121403	0.023805908
GBM	154	5	0.222631971	
HNSC	500	44	2.51E-05	4.38E-05
KICH	65	24	0.002037694	0.003035546
KIRC	530	72	0	5.22E-22
KIRP	288	32	2.54E-13	6.14E-13
LAML	151	0		
LGG	511	0		
LIHC	371	50	0	6.16E-19
LUAD	513	59	0	4.57E-23
LUSC	501	49	0	1.33E-18
MESO	86	0		
OV	374	0		
PAAD	177	4	0.351644062	0.314655376
PCPG	178	3	0.313984332	0.088238427
PRAD	495	52	0.642168337	0.604138831
READ	166	10	0.000888381	0.001242347
SARC	259	2		0.109963754
SKCM	103	1		
STAD	375	32	3.34E-07	2.69E-06
TGCT	150	0		
THCA	502	58	0.013749549	0.013634813
THYM	119	2		0.278652331
UCEC	543	35	0.012821788	0.0694288
UCS	56	0		
UVM	80	0		

Table S1 Differential DYRK2 expression analyses between tumor and matched normal tissues (where available) across all cancers in TCGA. (n= sample size)

	DYRK2-LDN192960
Data collection	
Space group	C 2 2 21
Cell dimensions (Å)	64.487, 129.127, 132.895
α, β, γ (°)	90, 90, 90
Wavelength (Å)	1.0000
Resolution (Å)	50-2.35(2.44-2.35)
CC1/2	0.995(0.824)
Rpim	0.044(0.339)
R_{merge}	0.155(1.115)
I / □I	24.6(3.0)
Completeness (%)	100.0 (100.0)
redundancy	13.2(11.5)
Wilson B-factor	31.14
Refinement	
No. reflections	23260
R_{work} / R_{free}	0.172 / 0.209
No. of atoms	
Protein	2649
Ligand/ion	23
Water	182
B-factors	
Macromolecules	36.58
Ligand/ion	36.24
Water	38.70
R.m.s deviations	
Bond lengths (Å)	0.008
Bond angles (°)	0.966
Ramachandran	
Favored (%)	94.04
Outliers (%)	0

Each dataset was collected from a single crystal. Values in parentheses are for highest-resolution shell.

Table S2 Co-crystallography data collection and refinement statistics.

SUPPLEMENTARY FIGURE LEGENDS

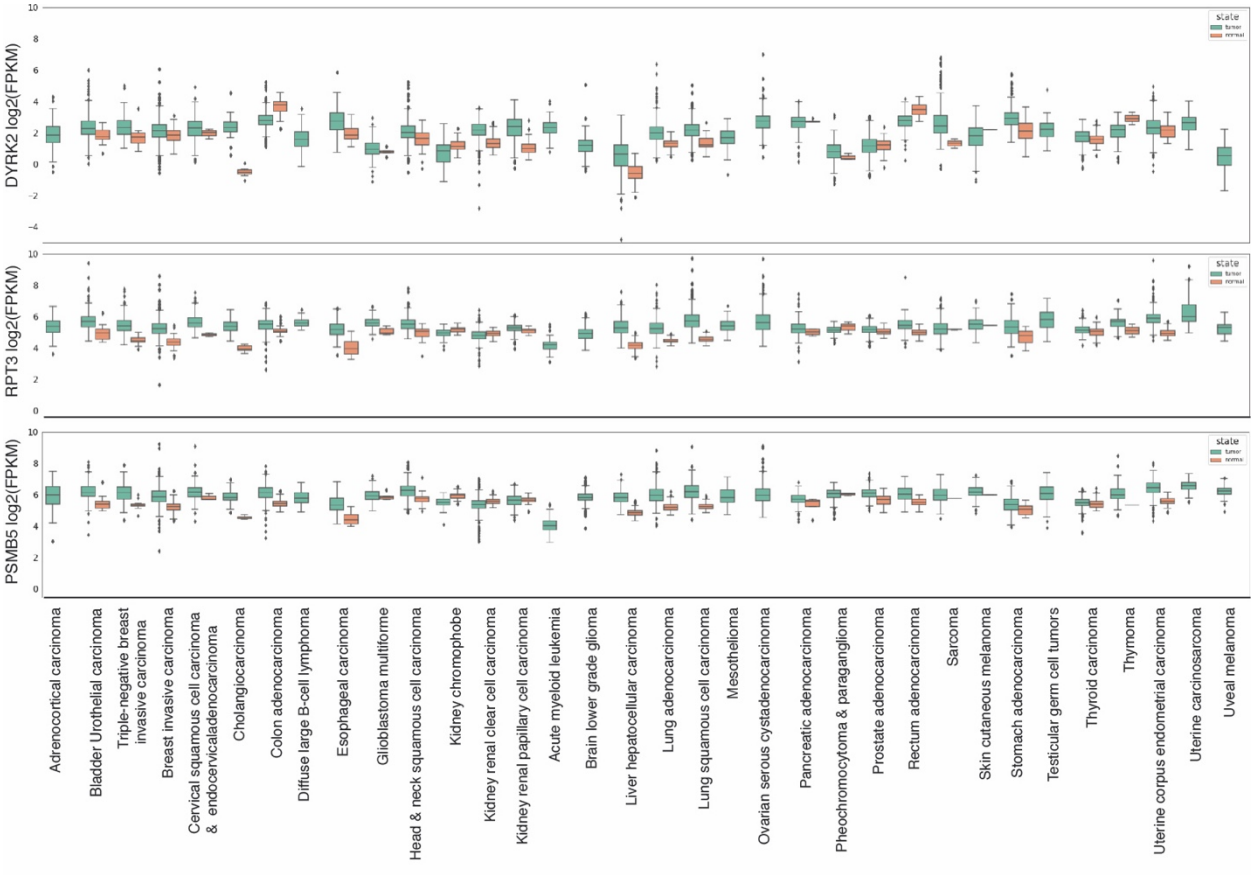

Figure S1. Differential gene expression analyses for DYRK2, RPT3, and PSMB5. The differential gene expression analyses were carried out for the indicated genes from the TCGA database. Data is represented as box-plots and p values were derived either with semi-paired modification (Derrick's) to the Student's t-test or standard Student's t-test. See also Table S1.

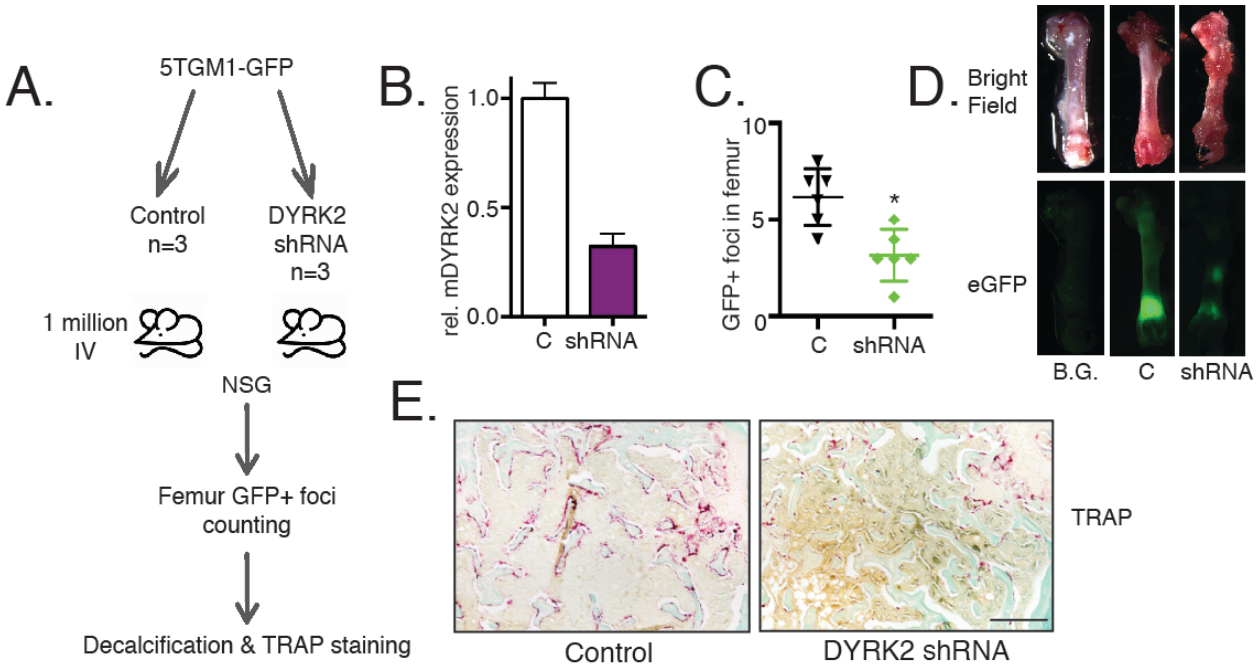

Figure S2. DYRK2 knockdown reduces GFP$^+$ foci and TRAP signal in 5TGM1-GFP/NSG^{TM} xenograft model.

(A) 5TGM1-GFP vector alone or shRNA knockdown of DYRK2 cells were injected intravenously into NSG^{TM} mice (n=3 per condition). 3 wk post injection, mice were euthanized and femur bone was excised.

(B) DYRK2 knockdown efficiency in 5TGM1-GFP cells as seen by qRT-PCR.

(C) Enumeration of GFP$^+$ foci. *$p<0.05$ (vector alone vs DYRK2 shRNA, unpaired Student's t-test, mean ± SD from n=3 mice each).

(D) Representative images of GFP$^+$ foci in mouse femurs (B.G.=background fluorescence).

(E) TRAP staining on the cross-sections of the fixed, decalcified femurs from 5TGM1-GFP/NSG^{TM} xenograft model.

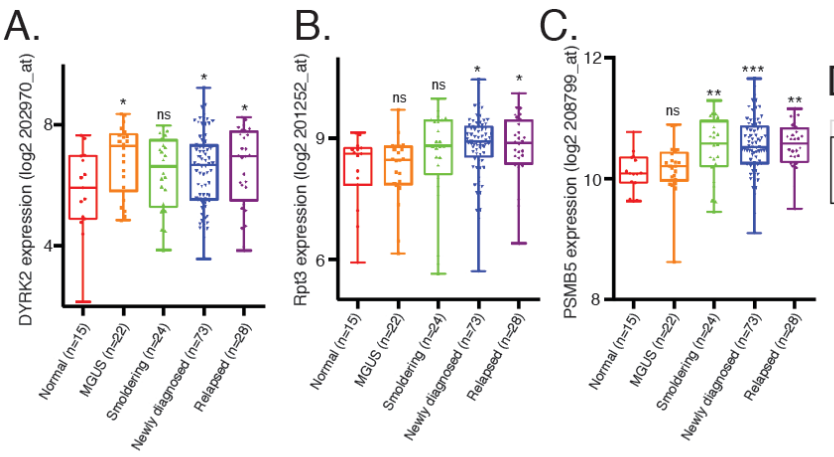

D.

p-value table		*DYRK2*	*Rpt3*	*PSMB5*
Normal *vs*	MGUS	*0.0105*	0.8546	0.6643
	Smoldering	0.1299	0.2234	*0.0081*
	Newly diag.	*0.0403*	*0.0137*	*0.0005*
	Relapsed	*0.0453*	*0.0497*	*0.0029*

Figure S3. Differential gene expression analyses for DYRK2, RPT3, and PSMB5 in various stages of multiple myeloma.

(A) DYRK2, (B) RPT3, and (C) PSMB5 differential gene expression analyses were performed on the multiple myeloma dataset with the accession number GSE6477 available at the Gene Expression Omnibus (GEO). Data is represented as box+scatter-plots and p values derived from empirical Bayes estimation on linear models of gene expression in *limma* package.

(D) Statistical p values shown in table.

A

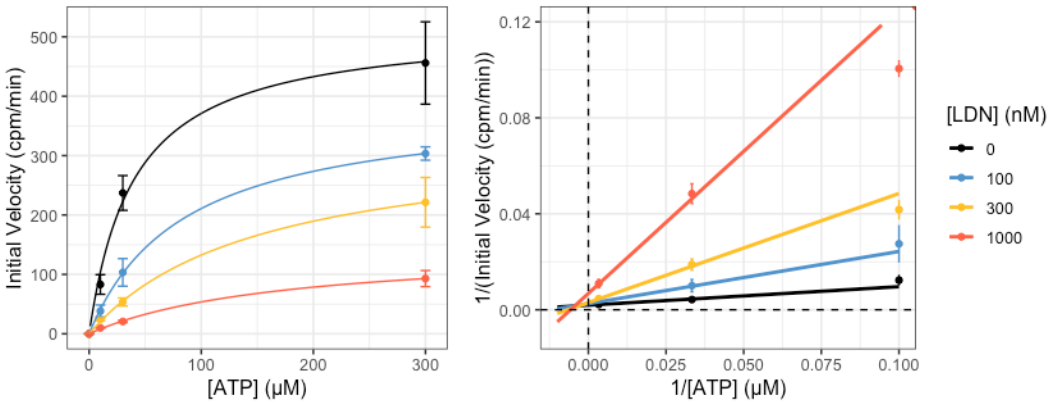

B

[LDN] (nM)	Vmax^{app}	Km^{app}
0	519 ± 31.7	40 ± 7.87
100	389 ± 16.6	84.6 ± 10.9
300	333 ± 49.1	151 ± 57.1
1000	147 ± 25.3	174 ± 75.2

Figure S4. Inhibitory mechanism of LDN192960 against DYRK2. (A) Michaelis-Menten (left) and Lineweaver-Burke (right) plots of full-length DYRK2 activity against woodtide under a variety of LDN192960 concentrations. Error bars denote standard deviation, n=3. (B) Apparent Vmax (CPM/minute) and Km (μM) values for Michaelis-Menten best fits at indicated LDN192960 concentration. Error indicates standard error of the nonlinear least squares fit.

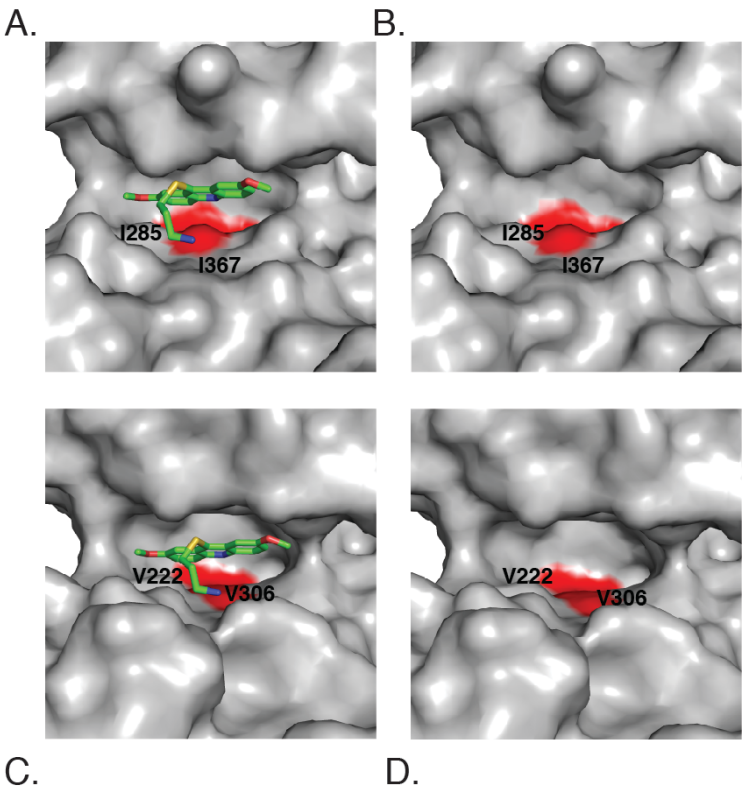

Figure S5. Comparison of LDN192960 docking site between DYRK2 and DYRK1.
(A) LDN192960 binds to the DYRK2 ATP-binding pocket in the co-crystal structure.
(B) Ile285 and Ile367 in DYRK2 form hydrophobic interactions with LDN192960 and are critical for the binding specificity.
(C) A structural model of LDN192960 binding to DYRK1A is generated based on the DYRK2-LDN192960 structure.
(D) DYRK1A has two valines at the positions corresponding to DYRK2 Ile285 and Ile367, the smaller side chains of which would lead to reduced binding to LDN192960.

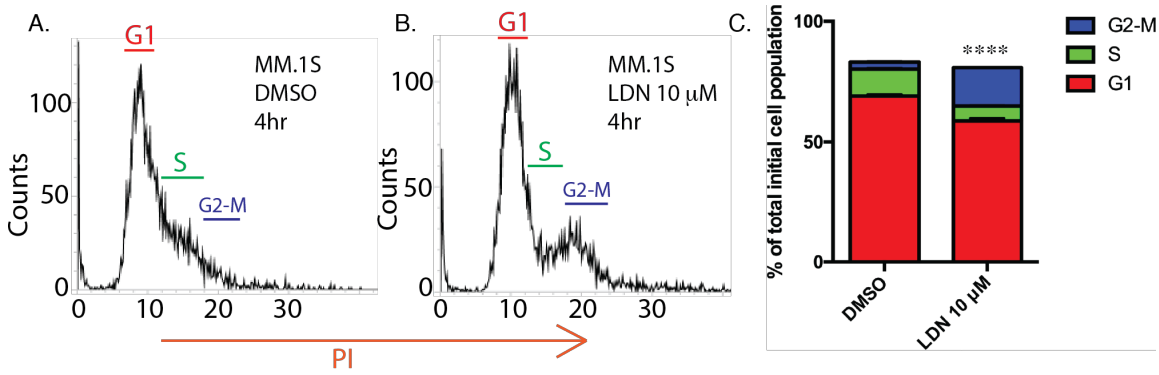

Figure S6. Cell cycle analyses for MM.1S cells treated with DMSO or LDN 10 μM for 4hr.

(A) MM.1S cells treated with DMSO control were fixed, permeabilized and stained with 50 μg/mL propidium iodide and cell cycle distribution was analysed by flow cytometry. Representative histogram is shown.

(B) Same as (A) except cells were treated with 10 μM LDN.

(C) Percentage of total initial cell populations in G1/S/G2-M stages are quantified in stacked bar graph (****$p<0.0001$).